Dr. M. P. Singh, 2026, 14:1
ISSN (Online): 2348-4098
ISSN (Print): 2395-4752

International Journal of Science, Engineering and Technology
An Open Access Journal

The inclusion of multiple parabolic sub-bands in thermoelectric transport coefficient of rectangular Bismuth Nano wires on the basis of Boltzmann relaxation time approach

Dr. M. P. Singh
Physics Department Rajkiya Mahila Mahavidyalaya Shahganj Jaunpur
Veer Bahadur Singh Purvanchal University Jaunpur Uttar Pradesh (INDIA).

Abstract- In the paper, we have generalized the formulation of the thermoelectric coefficients of rectangular nanowires based on the Boltzmann relaxation time approach. The relaxation time is energy-dependent due to multiple scattering phenomena, and with certain assumptions for the size quantum limit (SQL), transport coefficients are simplified for acoustic phonon scattering. For pure acoustic phonon scattering below 200 K, the Seebeck coefficient of bismuth nanowires changes from a maximum value to a minimum value in the range of 180-206 μV/K. The consideration of the multi-sub-band effect decreases the value of the Seebeck coefficient. The Wiedemann–Franz law is violated, and the Lorentz factor shows unexpected oscillatory behaviour below 200 K. The relaxation rate of the bismuth nanowire is $\tau = \tau_0 \varepsilon^{0.72}$.

Keywords: nano-structures, electronic transport, quantum wires.

I. INTRODUCTION

The thermoelectric transport coefficient is useful for categorizing thermoelectric materials and their industrial applications, such as power generation, refrigeration, and nanoscale medical and military equipment[1-10]. During the past two decades interest in low-dimensional structures has seen an upsurge of activity. As we reduce the size of the material and move to the nanoscale, the material's behaviour changes due to multiple complex processes. When restricted dimension's size is of the order of the de'Brogli wavelength of the confined carriers then quantum size effects are dominant; such a wave guide with cross-sectional size of the order of de'Brogli wavelength is known as quantum wire.

For observation of quantum size effects thermal energy of carriers must be less than energy level separation ( ). Since quantum size effects depend on the coherence of carriers, any scattering is likely to destroy quantum effects. The carrier mean free path must be greater than the size of the transverse confinement. An idealized thermoelectric material can be termed as PGEC (phonon glass electron crystal), and in any realistic situation one can keep in mind the ultimate ideal[11-23]. In addition to the search for conventional materials with high figure-of-merit a possibility of enhancing it by utilizing favourable thermal and electrical properties in two and one dimensions was seriously considered. Quantum wells, quantum wires and quantum dots have been the subject of intense theoretical and experimental research activity and its impact on thermoelectric technology is certain to emerge. At the theoretical level an improvement of thermoelectric conversion efficiency requires detailed knowledge of all the factors that determine their properties.

An understanding of the basic concepts such as electronic band structures and phonon dispersion relations are essential and useful in optimization programmes. Currently, nanowires have potential uses in thermoelectric transport phenomena, electronics, and optoelectronics. Nanowires exhibit low thermal conductivity. Due to enhanced numbers of interfaces and random atomic arrangements, they represent enhanced disorder. Consequently, the effective number of conduction electrons is limited to those that pass through or tunnel through all the

boundaries along the mean free path. When the transverse dimension of the nanowire is on the order of the mean free path, this enhances N-process electron-phonon and electron-electron scattering at low temperatures due to surface boundary collisions. As a result, the Wiedemann–Franz law is violated, and the Lorentz factor shows unexpected behaviour[24-34].

In this paper, we formulate the thermal transport coefficient for rectangular nanowires beyond the size quantum limit.

II. THEORY

An ideal one-dimensional electron gas differs from free electrons in bulk because the electrons have unrestricted movement in only one dimension, with complete confinement in the x and y directions. The system under consideration is a wire of length L along the z-axis, with a rectangular cross-section characterized by transverse dimensions 'a' and 'b'. The electronic wave function and energy eigenvalues are given by [7,25,26]

$$\psi_{nlk} = \frac{2}{\sqrt{abL}} \sin\left(\frac{n\pi x}{a}\right) \sin\left(\frac{l\pi y}{b}\right) e^{ik_z z} \quad (1)$$

$$E = n^2 \frac{\pi^2\hbar^2}{2m_x^* a^2} + l^2 \frac{\pi^2\hbar^2}{2m_y^* b^2} + \frac{\hbar^2 k_z^2}{2m_z^*}$$

$$E = E_n + E_l + \varepsilon \quad (2)$$

where n,l are nonnegative integer. Here k_z is the wave vector along z-direction, and m_x^*, m_y^* and m_z^* are the carrier effective masses along x, y and z-directions. The carrier energy along z-direction varies quasi-continuously.

$$\epsilon = E - E_n - E_l \quad (3)$$

Transport coefficients for a quasi-one-dimensional system, such as a nanowire, may be obtained using the familiar Boltzmann equation approach. For a quasi-one-dimensional system (Q1D), the transport coefficients, such as electrical conductivity, Seebeck coefficient, and the electronic contribution to thermal conductivity, can be written as follows: [2,3]

$$\sigma = \frac{e^2}{T}\Gamma^1 \quad (4)$$

$$\alpha = \frac{E_F}{eT} + \frac{1}{eT}\frac{\Gamma^2}{\Gamma^1} \quad (5)$$

$$k_e = \frac{1}{T}\Gamma^3 - \frac{1}{T}\sigma\left(\alpha T - \frac{E_F}{e}\right)^2 \quad (6)$$

The transport coefficient may be derived by semi-classical approach in which particles are confined in two dimensions (x and y). Thermal gradient is present along z-direction, whereas x and y-directions are the confined directions. The transport coefficients for quasi one-dimensional system (Q1D) may be written as $\Gamma^1 = -\zeta^{(0)}$; $\Gamma^2 = \zeta^{(1)}$; $\Gamma^3 = -\zeta^{(2)}$ Functions $\zeta^{(s)}$ can be written as

$$\zeta^{(s)} = \frac{T}{2\pi ab}\left(\frac{2m_z^*}{\hbar^2}\right)^{\frac{3}{2}}\left(\frac{\hbar}{m_z^*}\right)^2 \sum_{n,l=1,0} \int E^s \varepsilon^{\left(\frac{1}{2}\right)} \tau \left(\frac{\partial f}{\partial \varepsilon}\right) d\varepsilon \quad (7)$$

The relaxation time for acoustic phonon scattering in one-dimensional systems is essentially energy dependent and is given by [28]

$$\tau_{nl}(k) = \frac{4}{9}\frac{\hbar^2 c_{11} ab}{2\varepsilon_1^2 (k_B T)(2m^*)^{\frac{1}{2}}} \varepsilon^{\frac{1}{2}}$$

For three-dimensional system the relaxation time τ will be taken to have form [3]

$$\tau = \tau_0 (E - E_c)^p$$

For lattice scattering $p = -\frac{1}{2}$ and for ionized impurity scattering $p = \frac{3}{2}$

On the account of above reference, we assume that the relaxation time τ for nanowire are given by the expression

$$\tau = \tau_0 \varepsilon^p \quad (8)$$

With this approximation's expressions of Electrical conductivity, Seebeck coefficient, can be written as

$$\sigma = \frac{2\tau_0 e^2}{\pi\hbar ab(2m_z^*)^{1/2}} B_6 \quad (9)$$

The ratio electronic contribution to thermal conductivity and; product of temperature and electrical conductivity; are given by equation k_e/σT=L where L is called Lorentz number. L=(k_B/e)^2 L_f .Here Lorentz factor L_f .The electronic contribution to thermal conductivity may be written as [2,3]

$$\alpha = \frac{k_B}{e}\left[\frac{E_F}{k_B T} - \frac{B_4 + B_5}{k_B T B_6}\right] \quad (10)$$

The ratio electronic contribution to thermal conductivity and; product of temperature and electrical conductivity; are given by equation $\frac{k_e}{\sigma T} = L$

where L is called Lorentz number $L = \left(\frac{k_B}{e}\right)^2 L_f$ L_f .Here Lorentz factor L_f .The electronic contribution to thermal conductivity may be written as [2,3]

$$k_e = \left(\frac{k_B}{e}\right)^2 L_f \sigma T \quad (11)$$

Lorentz factor Lf for Q1D system may be written as

$$L_f = \left[\frac{B_1+2B_2+B_3}{(k_BT)^2 B_6} - \left(\frac{B_4+B_5}{k_BTB_6}\right)^2\right] \quad (12)$$

where B_1, B_2, B_3, B_4, B_5, and B_6 are given by

$$B_1 = \sum_n \sum_l \left(p+\frac{5}{2}\right)(k_BT)^{\left(p+\frac{5}{2}\right)} F_{\left(p+\frac{3}{2}\right)}(\eta_{n,l}) \quad (13)$$

$$B_2 = \sum_n \sum_l (E_n' + E_l')\left(p+\frac{3}{2}\right)(k_BT)^{\left(p+\frac{5}{2}\right)} F_{\left(p+\frac{1}{2}\right)}(\eta_{n,l}) \quad (14)$$

$$B_3 = \sum_n \sum_l (E_n' + E_l')^2 \left(p+\frac{1}{2}\right)(k_BT)^{\left(p+\frac{5}{2}\right)} F_{\left(p-\frac{1}{2}\right)}(\eta_{n,l}) \quad (15)$$

$$B_4 = \sum_n \sum_l \left(p+\frac{3}{2}\right)(k_BT)^{\left(p+\frac{3}{2}\right)} F_{\left(p+\frac{1}{2}\right)}(\eta_{n,l}) \quad (16)$$

$$B_5 = \sum_n \sum_l (E_n' + E_l')\left(p+\frac{1}{2}\right)(k_BT)^{\left(p+\frac{3}{2}\right)} F_{\left(p-\frac{1}{2}\right)}(\eta_{n,l}) \quad (17)$$

$$B_6 = \sum_n \sum_l \left(p+\frac{1}{2}\right)(k_BT)^{\left(p+\frac{1}{2}\right)} F_{\left(p-\frac{1}{2}\right)}(\eta_{n,l}) \quad (18)$$

where $F_{(p)}(\eta_{n,l})$ is Fermi-integral defined as

$$F_{(p)}(\eta_{n,l}) = \int_0^\infty \frac{x^p}{\exp(x-\eta_{n,l})+1} dx \quad (19)$$

$E_n' = \frac{E_n}{k_BT}$ $E_l' = \frac{E_l}{k_BT}$, reduced carrier energy $x = \frac{\varepsilon}{k_BT}$ with respect to conduction band edge, $\eta_{n,l} = \xi - E_n' - E_l'$; reduced Fermi energy $\xi = \frac{E_F}{k_BT}$. Here summation taken over several sub-bands

CASE1:

Some simplifying assumptions are often considered to facilitate the calculations. Taking p=0 amounts to considering electron relaxation rate to be independent of carrier energy. Another assumption oversimplifies the summation over n and l by assumption all electron is assume to in lowest sub-bands n=l=1 With this assumption the electrical conductivity, Seebeck coefficient and Lorentz factor are given by

$$\sigma = \frac{\tau_0 e^2}{\pi ab\hbar}\left(\frac{k_BT}{2m_z}\right)^{\frac{1}{2}} F_{-\frac{1}{2}}(\eta_{11}) \quad (20)$$

$$\alpha = \frac{k_B}{e}\left[\eta_{11} - \frac{3F_{\frac{1}{2}}(\eta_{11})}{F_{-\frac{1}{2}}(\eta_{11})}\right] \quad (21)$$

$$L_f = \left[\frac{5F_{\frac{3}{2}}(\eta_{11})}{F_{-\frac{1}{2}}(\eta_{11})} - \left(\frac{3F_{\frac{1}{2}}(\eta_{11})}{F_{-\frac{1}{2}}(\eta_{11})}\right)^2\right] \quad (22)$$

CASE2:

It is possible to go beyond the simplifying assumptions the relaxation time for acoustic phonon scattering in one-dimensional systems is essentially energy dependent and is given by [28]

$$\tau_{nl}(k) = \frac{4}{9}\frac{\hbar^2 c_{11} ab}{2\varepsilon_1^2 (k_BT)(2m^*)^{\frac{1}{2}}}\varepsilon^{\frac{1}{2}} \quad (23)$$

Here is the longitudinal elastic constant and is the deformation potential. Within the limitation of the size quantum limit (SQL) but with a better choice for the carrier relaxation time, we obtain following expression taking (a=b)

$$\sigma = \frac{2\hbar c_{11} e^2}{9\pi m_z^* \varepsilon_1^2} F_0(\eta_{11}) \quad (24)$$

$$\alpha = \frac{k_B}{e}\left[\eta_{11} - \frac{2F_1(\eta_{11})}{F_0(\eta_{11})}\right] \quad (25)$$

$$L_f = \left[\frac{3F_2(\eta_{11})}{F_0(\eta_{11})} - \left(\frac{2F_1(\eta_{11})}{F_0(\eta_{11})}\right)^2\right] \quad (26)$$

Dresselhaus et al. have obtained expressions for transport coefficients that are in agreement with our expressions for a particular relaxation time and SQL [29-30]. The expressions for the transport coefficients of rectangular nanowires (Equations 9, 10, 11,12,13,14,15,16,17,18 and 19) are significant landmarks in the field of thermal transport research. By varying the energy-dependent parameter p of the relaxation time, experimental physicists may identify different scattering mechanisms. Due to two-dimensional confinement, multiple parabolic sub-bands arise, and the number of bands actively participating in the transport of energy and current can be identified from the above expressions.

III. RESULT AND DISCUSSION

The theoretical model described here has been applied to bismuth nanowires because very large anisotropy of three ellipsoidal constant energy surface at L point in the rhombohedral Brillouin zone ,high mobility of carriers and small electron effective mass component, quantum confinement effect in the nanowires are more prominent as compare to other wire at same size. Bi has carries with very long mean free path for electronic transportation and heavy mass ions, which are more effective for phonon scattering. Semi metal-Semiconductors transition occurs in Bi nanowire at 49nm and 77K, lowest conduction sub-band edge formed by the L electrons crosses highest T-point valence sub-band. Bi nanowire are more useful for thermoelectric application transport phenomenon dominated by single type of carrier electrons or holes only and electro chemical potential is placed to achieve optimum ZT[7,34].

Figures 1a and 1b illustrate the variation of the Seebeck coefficient for 50 nm and 100 nm bismuth nanowires along the trigonal axis, considering acoustic phonon scattering and the multi-sub-band effect. Figure 1c shows variation of Seebeck coefficient versus reduced fermi energy at temperature 77K and cross-sectional size 50nm along Bi nanowire oriented along trigonal principal axes including effect of sub-band quantisation for acoustic phonon scattering.

For both 50 nm and 100 nm nanowires, the Seebeck coefficient maxima shift toward higher temperatures when the multi-sub-band effect is included in the transport calculations. The maxima are broad and flat for 50 nm nanowires, while they are sharp for 100 nm nanowires. For 50 nm nanowires, some minima appear at lower temperatures. For instance, a minimum appears around 60 K in the '^' data4.

The mode (n,m) = (1,1) indicates that all sub-bands below or equal to (1,1) have been considered (+ dtata1). The mode (n,m) = (2,2) indicates that all sub-bands below or equal to (2,2) have been considered (* data2). The mode (n,m) = (3,3) indicates that all sub-bands below or equal to (3,3) have been considered (x data3). The mode (n,m) = (4,4) indicates that all sub-bands below or equal to (4,4) have been considered (^ data4).

Below 250 K, bismuth nanowires undergo a transition from semi-metallic to semiconducting behaviour. The Seebeck coefficient ranges from 180 to 206 μV/K.

Calculated value of Seebeck Coefficient(μV/K) of Bi nanowire oriented along trigonal and binary principal axes of rectangular size 40nm at 77K including effect of sub-band quantisation shown in table-01.

Figures 2a and 2b illustrate the variation of the Lorentz factor with temperature for 50 nm and 100 nm Bismuth nanowires, considering acoustic phonon scattering and multiple sub-bands. Figure 2c shows variation of Lorentz Factor versus reduced fermi energy at temperature 77K and cross-sectional size 50nm along trigonal axes of Bismuth nanowire for acoustic phonon scattering.

The Lorentz factor for Bismuth nanowires exhibits both maxima and minima as a function of temperature. Below 250 K, Bismuth nanowires exhibit a semiconducting-conducting phase transition, with the Lorentz factor ranging from 2.2 to 2.5. As the cross-sectional width increases, the maxima and minima become sharper, and the distance between them decreases. Additionally, as the number of modes increases, the maxima shift towards higher temperatures. Calculated value of dimensionless Lorentz Factor of Bi nanowire oriented along trigonal and binary principal axes of rectangular size 40nm at 77K including effect of sub-band quantisation.

Figure 3 shows that at low temperatures, relaxation is due to a combined scattering mechanism. As the temperature increases, other scattering mechanisms play a significant role. Since the experimental results are very close to the '^' data 3 line at 10 K and follow the path between the '*'data2 line and '^' data 3 lines, the theoretical model of Bi nanowires is in good agreement with the experimental results. This indicates that, along with acoustic phonon

scattering, other scattering mechanisms also play a minor role in the relaxation rate of bismuth nanowires. This is due to the quantum confinement of the carrier pockets.

IV. CONCLUSION

The conclusions can be drawn from the present studies: Equations 9 to 19 are generalized formulas for nanowires based on the Boltzmann Relaxation approach, including the multi-sub-band effect. For pure acoustic phonon scattering 〖τ=τ〗_0 ε^0.5, it was observed that 〖τ=τ〗_0 ε^0.72. This means that surface boundaries play a significant role in the nanowire. Below 200 K, the Seebeck coefficient of bismuth nanowires changes from a maximum to a minimum value in the range of 180-206 μV/K. Consideration of the multi-sub-band effect lowers the value of the Seebeck coefficient. The Wiedemann-Franz law is violated, and the Lorentz factor shows unexpected oscillatory behaviour below 250 K. For more accurate model of Bi nanowire of other shapes such as circular, hexagonal etc. should be considered for further study. Since electron motion are allowed only along the wire axes electron expected to behave like 1D electron system with non-parabolic dispersion relation. The non-parabolic feature of the L-point conduction band and temperature dependence various band parameter change.

V. FIGURE CAPTION

Fig1a: Bismuth nanowire 50nm along trigonal axes Seebeck coefficient for acoustic phonon scattering (n,m)=(1,1)(+data1); (2,2) (*data2); (3,3) (x data3); (4,4) (^data4)

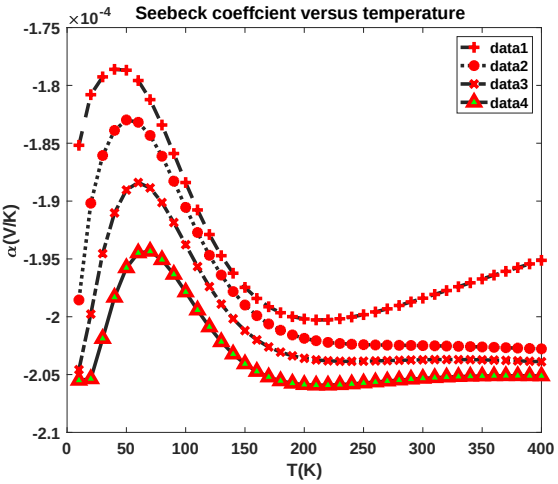

Fig1b: Bismuth nanowire 100nm along trigonal axes Seebeck coefficient for acoustic phonon scattering (n,m)=(1,1) (+data1); (2,2) (*data2); (3,3) (x data3); (4,4) (^data4)

Fig1c: Figure shows variation of Seebeck coefficient versus reduced fermi energy at temperature 77K and cross-sectional size 50nm along Bi nanowire oriented along trigonal principal axes including effect of sub-band quantisation for acoustic phonon scattering. Mode (n,m) means all sub-band below the (n,m) actively participate (n,m)=(1,1) (+ data1); (2,2) (* data2); (3,3) (x data3); (4,4) (^data4).

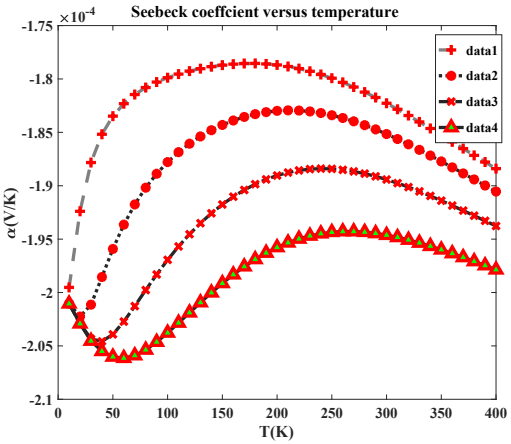

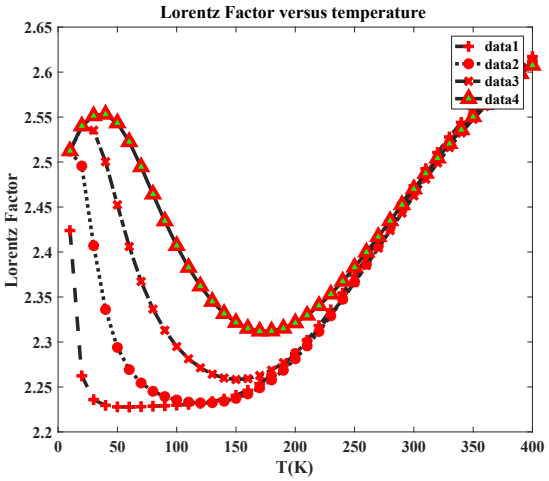

Fig2a: Bismuth nanowire 50nm along trigonal axes Lorentz Factor for acoustic phonon scattering (n,m)=(1,1) (+ data1); (2,2) (* data2); (3,3) (x data3); (4,4) (^data4)

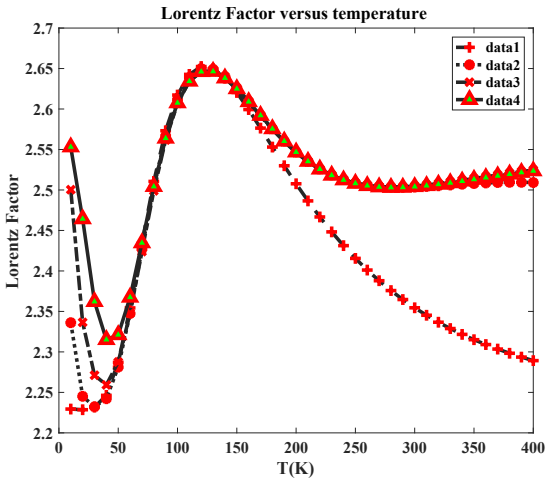

Fig2b: Bismuth nanowire 100nm along trigonal axes Lorentz Factor for acoustic phonon scattering (n,m)=(1,1) (+ data1); (2,2) (* data2); (3,3) (x data3); (4,4) (^data4)

Fig2c: Figure shows variation of Lorentz Factor versus reduced fermi energy at temperature 77K and cross-sectional size 50nm along trigonal axes of Bismuth nanowire for acoustic phonon scattering (n,m)=(1,1) (+ data1); (2,2) (* data2); (3,3) (x data3); (4,4) (^data4)

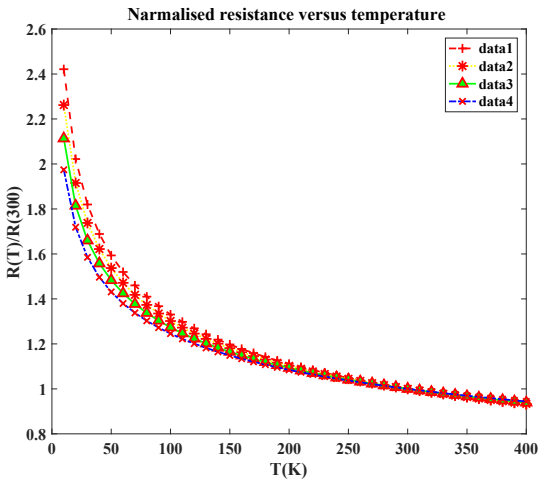

Fig3: Bismuth nanowire 48nm along trigonal axes (n,m)=(1,1) resistance for p=0.76(+ data1); 0.74 (* data2); 0.72(^ data3); 0.70 (x data4).

Table-01 Calculated value of Seebeck Coefficient(μV/K) of Bi nanowire oriented along trigonal and binary principal axes of rectangular size 40nm at 77K including effect of sub-band quantisation. Mode (n,m) means all sub-band below the (n,m) actively participated in transportation in energy.

Direction	Reduced Fermi energy	Mode (n,m) =(1,1)	Mode (n,m) =(2,2)	Mode (n,m) =(3,3)	Mode (n,m) =(4,4)
Trigonal axes	-1	283	296	303	305
	0	213	262	233	236
	1	158	170	178	180
Binary axes	-1	277	286	296	303
	0	209	217	226	233
	1	154	161	169	176

Table:02 Calculated value of dimensionless Lorentz Factor of Bi nanowire oriented along trigonal and binary principal axes of rectangular size 40nm at 77K including effect of sub-band quantisation.

Direction	Reduced Fermi energy	Mode (n,m)=(1,1)	Mode (n,m)=(2,2)	Mode (n,m) =(3,3)	Mode (n,m)=(4,4)
Trigonal axes	-1	2.08492	2.2028	2.3748	2.4541
	0	2.1665	2.2557	2.4219	2.5064
	1	2.3021	2.3469	2.4969	2.5895
Binary axes	-1	2.0753	2.1001	2.1806	2.3015
	0	2.165	2.1752	2.2360	2.3458
	1	2.308	2.3024	2.3329	2.4192

V. REFERENCE

1. C.M. Bhandari, CRC Handbook of Thermoelectrics Edited by D.M. Rowe chap-4, 5, 6(1995).
2. J.M. Ziman, Electrons and phonons "Theory of transport phenomena of solid"(oxford At The Clarendon Press) 385(1960)
3. J.R. Drabble, H.J. Goldsmid, Thermal Conduction in Semi- conductors, (Pergaman Press, London,) 105-109(1961).

4. G. S. Nolas, J. Sharp, and H. J. Goldsmid "Thermoelctrics-Basic Principles and New Material Development" (Springer Series in Materials Science)-45 (2001).
5. C. W. J. Beenakker and H. V. Houten, "Quantum transport in Semiconductor Nanostructures", Solid State Physics: Advanced in Research and Application, (Acedemic Press Inc SanDiego USA) edited by Henery Ehrenreich and David Turnbull, 44 (1991).
6. M. S. Dresselhaus etal, "Quantum wells and quantum wires for potentials thermoelectric Application" Resent Trends in Thermoelectric Materials, Research III, Semiconductor and Semimetals, (Academic Press,) Editor. Terry M. Tritt 61-71 (2001)
7. E. A. Johnson, Electron in quantum semiconductor structures in "Low-dimensional Semiconductor structures" Edited by Barnham K and Vvdensky D, Cambridge University Press, chapter-2, 4 and 6.
8. Rosas Rodrigo, Riera Raul, Marin Jose L and Compoy German "Handbook of thin film Materials" edited by Hari Singh Nalwa, Academic Press San Diego USA vol-5 cha-06 (2002).
9. Xue, Haoran, Yihao Yang, and Baile Zhang. "Topological acoustics." Nature Reviews Materials 7.12 ,974 (2022)
10. G. A. Slack 'New materials and Performance Limits for thermoelectric cooling'. In CRC Handbook of Thermoelectrics; Rowe D.M. (Ed.), CRC Press: Boca Raton, FL,1995, 407-440.
11. G. D. Mahan, "Good Thermoelectrics" in Solid State Physics edited. by H. Ehrenreich and F. Saepen Academic Press, San Diego, 51(1998).
12. R. Venkatasubramanian , E.Siivola, T. Colpitts and B. O'Quinn, Nature 413, 597(2001).
13. C.W.J Beenakker and H. V. Houten, "Quantum transport in Semiconductor Nanostructures", Solid State Physics: Advanced in Research and Application, edited by Henery Ehrenreich and David Turnbull, Acedemic Press Inc SanDiego USA 44 (1991).
14. M.F.P.Wagner, A.S. Paulus, W.Sigle, et al. Sci Rep 13, 8290 (2023).
15. Hernandez, J.A., Ruiz, A., Fonseca, L.F. et al. Sci Rep 8, 11966 (2018). https://doi.org/10.1038/s41598-018-30450-5
16. Lin Yong, Huh daihong etal. Nature communication 12,3926(2021)
17. M. P. Singh 2018 J. Phys. Commun. https://doi.org/10.1088/2399-6528/aaaee3
18. X. Wang, J.Young etal .Measurement of science and Technology 29(2), 025001(2018)
19. Jeongmin Kim, Wooyoung Shim and Wooyoung Lee, Journal of Materials Chemistry C. 3, 11999 (2015) doi:10.1039/c5tc02886h
20. Jose A. Hernandez etal Scientific Report 8,11966(2018)
21. M. N. Ou, T. J. Yang etal. Applied physics Letters 92, 063101(2008). Doi.10.1063/1.2839572
22. Hochbaum, et al. Nature 451, 163 (2008).
23. Khitun, K L Wang and G Chen, Nanotechnology 11, 327(2000).
24. M. P. Singh and C.M. Bhandari, Pramana: Journal of Physics 62, No.6, 1309(2004)
25. M. P. Singh and C. M. Bhandari, Indian Pure and Applied Physics 41, 950(2003)
26. M. P. Singh and C.M. Bhandari, Solid State Communications 133,29 (2005)
27. M.P. Singh and C. M. Bhandari, Solid St Comm 127, 649 (2003). https://doi.org/10.1016/S0038-1098(03)00520-9
28. J. Lee and M.O. Vassell , J. Phys C :Solid State Phys 17,2525 (1984).
29. L. D. Hicks, and M. S. Dresselhaus, Phys. Rev. B,47,12727(1993)
30. L. D. Hicks, and M. S. Dresselhaus, Phys. Rev.B,47,16631(1993).
31. T.Ando ,A.B. Fowler, and F. Stern, Rev. Mod. Phys. 54, 437 (1982).
32. S. S. Kubakaddi , and B.G.Mulimani , J. Appl. Phys 58, 3643 (1985).
33. X. Sun, Z.Zhang, and M.S.Dresselhaus, Appl. Phys. Lett. 74, 4005(1999).
34. Z.Zhang, X. Sun, M. S. Dresselhaus ,J.Mater.Res.13. 1745(1998)